Fault Detection on Large Slow Bearings

Eric Bechhoefer[1], Rune Schlanbusch[2] and Tor Inge Waag[3]

[1]*GPMS Inc, Cornwall, VT, USA*
eric@gpms-vt.com

[2]*Teknova AS, Kristiansand, Norway*
rune.schlanbusch.2008@ieee.org

[3]*MHWirth AS, Kristiansand, Norway*
tor.waag @mhwirth.com

ABSTRACT

Large, slow turning bearings remain difficult to analyze for diagnostics and prognostics. For critical equipment, such as drilling equipment, top drives, mining equipment, wind turbine main rotors, helicopter swash plates, etc. this poses safety and logistics support problems. An undetected bearing fault can disrupt service, and causes delays, lost productivity, or accidents. This paper examines a strategy for analysis of large slow bearings to improve the fault detection of condition monitoring systems, thus reducing operations and maintenance cost associated with these bearing faults. This analysis was based on vibration, temperature and grease analysis from three wind turbines, where one turbine was suspected of having a faulted main bearing.

1. INTRODUCTION

This paper looks at a number of techniques in the diagnostics of large, slow turning bearings. Specifically, the use of: vibration, temperature and grease analysis from three wind turbine main bearings. This analysis was initiated as one machine is suspected of having a main bearing fault. The primary focus of the analysis is vibration based.

1.1. Fundamentals of Bearing Analysis

Large, slow rotating bearings are based on a rolling element bearing design. They are common in all large rotating machines and one of the most frequent reasons for machine failures. In general, because roller element bearings are so fundamental to rotating machines, their vibration signals have been widely studied.

The benchmark for bearing diagnostics is the envelope analysis (Darlow, Badgley & Hogg et al., 1974). This is because the spectrum of a raw signal often contains little diagnostics information about bearing faults. The envelope analysis is based on a bandpass filtering around a high frequency band in which the fault impulses are amplified by structural resonance. The signal is then amplitude demodulated, and the spectrum of this envelope signal contains the diagnostics information.

When a rolling element strikes a local fault (or the rolling element fault hits the inner or outer race), an impact is produced on the structure. The resonance is a result of the natural frequency of the bearing/support structure. The modulation rate is associated with the bearing pass frequency, such as:

- Cage Pass Frequency (CPF):

$$f_{CPF} = f_r \tfrac{1}{2}\left(1 - BD/PD\ cos(\beta)\right), \quad (1)$$

- Ball Fault Frequency (BFF):

$$f_{BFF} = f_r\, {PD}/{BD}\left[1 - \left(BD/PD\ cos(\beta)\right)^2\right], \quad (2)$$

- Ball Pass Frequency Inner Race (BPFI):

$$f_{BPFI} = f_r\, {n}/{2}\left(1 + BD/PD\ cos(\beta)\right), \quad (3)$$

- Ball Pass Frequency Outer Race (BPFO):

$$f_{PBFO} = f_r\, {n}/{2}\left(1 - BD/PD\ cos(\beta)\right), \quad (4)$$

where n is the number of balls or rolling elements, f_r is the relative rate between inner and outer races (e.g. usually the shaft rate for a fixed bearing), PD is the pitch diameter (inner + outer race)/2, BD is the ball diameter, and β is the contact angle.

Consider the example inner race fault (Bechhoefer, 2013). The bearing roller diameter is 0.235 inches, pitch diameter of 1.245, with eight rolling elements and a contact angle of 0. The BPFI is 118.2 Hz, i.e. $f_{BPFI} = \mathrm{f_r}\times 4.7550$, with a shaft rate of $f_r = 25$ Hz. One revolution of the shaft takes 0.04 seconds, in which the inner race impact will be seen ~ four times, or in two revolutions (0.08 seconds), nine times (Figure **1**). The impacts are seen to be 1/BPFI in time, or spaced 0.0084 seconds. Of interest is that the magnitude of

the impacts varies with 1/Rev, as the inner race fault passes under the load zone of the bearing, where Rev is the number of revolutions over the sampling period. In the frequency domain, the 1/Rev modulation results in side bands around the fault frequency. This is an indicator of an inner race fault.

Zooming into one impact (time 0.0135 to 0.017), the resonance of the bearing structure is seen. Usually, there are a number of resonant modes. The period is approximately 0.0027 seconds, or a first mode of 380 Hz.

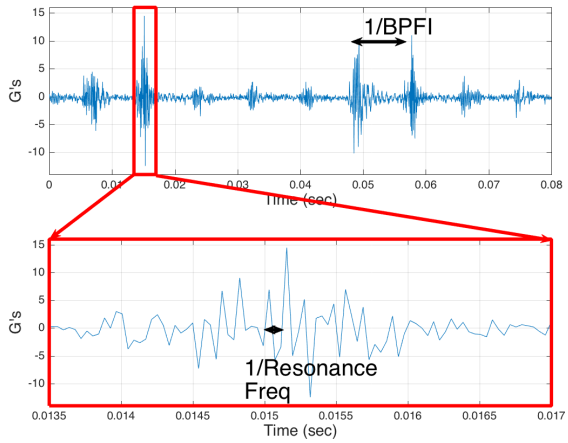

Figure 1. Inner Race Fault, Time Domain.

Over the intervening 40 years, a number of improvements to the envelope analysis have been made. In (Ho & Randall, 2000), the enveloped was calculated as the modulus of the analytic signal obtained by the inverse transformation of the selected one-sided frequency band. This was further improved upon in (Randall, 2011), with Matlab© pseudo code

1. X = fft(x); *%Take the FFT of the vibration signal*
2. dfrq = sample_rate/length(x); *%Get the freq. bin width*
3. idxLw = floor(22,000/dfrq); *%find the indexes of the*
4. idxHi = floor(24,000/dfrq); *%envelope window*
5. X(1:(idxHi-idxLw+1) =X(idxLw:idxHi);*%Heterodyne*
6. X((idxHi-idxLw+2):end) = 0; *%Hilbert Transform*
7. env = abs(ifft(X)); *% get the envelope*

The heterodyne process, line 5, copies and translates the window of interest to base-band, then low pass filters in the frequency domain, in one step. In line 6, the condition necessary to calculate the Hilbert transform is performed. Finally, the resulting envelope (env variable in line 7) is easily calculated as the absolute value of the inverse fast Fourier transform (FFT).

For embedded systems, Bechhoefer (2012) developed an envelope analysis with reduced computation complexity. Since there is a bandwidth reduction in the envelope, only those data points needed for the envelope should be processed. This was accomplished by low pass filtering and decimating in one step, then taking advantage of the trigonometric identity:

$$cos(a)\times cos(cf) = \tfrac{1}{2}[cos(a-cf) + cos(a+cf)], \quad (5)$$

which performs the heterodyne operation. Here *cf* is the center of the window frequency. For example, a structure with a resonance as 2.5 KHz, *cf* is 2.5 KHz. The high frequency image, *cos(a+cf)* will be filtered in the decimation process. The Hilbert transform was created by noting that the imaginary part of the Hilbert transform is the real part phase shifted by 90 degrees. Since *sin (cf+ π/2) = cos(cf)*, the imaginary part was created by multiplying the heterodyned signal by *sin(cf)*. In the heterodyne process, *sin(cf)* and *cos(cf)* are updated by the constant angle ω. This allowed the use of Clenshaw's recurrence algorithm, which removes most trigonometric function calls.

2. LARGE SLOW BEARING ANALYSIS

Large slow bearings present an analysis challenge due to three considerations: resolution, small acceleration feature and inexperience (e.g. lack of test data). These issues in one way relate to the nature of the operating environment.

2.1. Resolution

Resolution is the ability to discern one feature from another. Consider analysis of the main bearing of a commercial, 1.25 MW wind turbine. The main rotor shaft speed is approximately 20 revolutions per minute (RPM), or 0.34 Hz. The main bearing fault rates, as defined in Eq. (1)-(4) are given as $f_{CPF} = 0.45$, $f_{BFF} = 10.8$, $f_{BPFI} = 15.3$, and $f_{BPFO} = 12.7$. The respective frequencies of interest are: $[0.45\ 10.8\ 15.3\ 12.7] \times 0.34$ Hz which are 0.15, 3.67, 5.2 and 4.32 Hz.

Assume that one needs at least 10, preferable 30 bins between the frequencies of interest. To distinguish between direct current (DC) component, i.e. zeroth order, and f_{CPF}, the frequency resolution must be between 0.015 and 0.005 Hz.

For a sample rate of 3,000 samples per second (Nyquist of 1,500 Hz), this is 300,000 data points. Since the FFT typically uses radix 2, i.e. *2^ceil(log_2(300,000)*, or 524,288 data points, which is 175 seconds of data!

Of course, in most applications, the torque/load is not constant over time. In this wind turbine application, due to tower shadow and wind shear, there is a three per revolution change in speed (Figure 2).

In this two minute acquisition, the standard deviation of main rotor shaft speed is 0.0103 RPM, or 0.62 Hz. Numerically, this means that 68% of the time, given the 0.005 Hz/bin resolution, the spectral content is smeared

across +/-136 bins in the frequency domain. In order to correct for variation and shaft rate (f_r) and improve the envelope analysis, a time synchronous resampling algorithm was developed (Bechhoefer, Van Hecke & He, 2013).

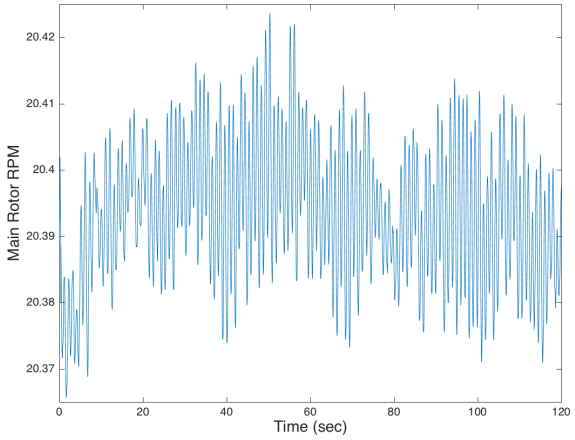

Figure 2. Main Rotor RPM over 120 Seconds.

This algorithm used a tachometer signal to phase lock the shaft under analysis, and resamples the vibration data into the spatial domain of the shaft. In this example, given the approximately 0.34 Hz shaft rate, it takes approximately 2.9 seconds for a revolution. For a sample rate of 3,000 samples per second (sps), there are, on average, 8,800 data points. In the resampling algorithm, for each revolution, the data is up-sampled to 16,384 data points. This effectively removes any variation in shaft speed.

2.2. Bearing Fault Features Energy

Faults associated with slowly rotating equipment are difficult to measure because the energy is small. Consider a 30 Hz output shaft, with a 0.001" (1 mil) displacement fault on the outer race (e.g. f_{BPFO} of 5). Because acceleration is the second derivative of displacement, the estimated acceleration of this fault would be 0.0511 (30 x 5)^2 x 0.001 = 1.15 Gs. This is not an unreasonable value, as we can see in Figure 1, an RMS of 1.76 Gs on a 25 Hz shaft.

For the wind turbine example, with $f_r = 0.34$ Hz and $f_{BPFO} = 4.3$ Hz, the same damage, 0.001", would generate an acceleration of $0.0511 \times 4.3^2 \times 0.001 = 0.00094$ Gs. This is a very small value to measure in the presence of noise.

2.3. Few Data Sets

Finally, there is a lack of experience in working with large bearings. There is little, if any, documentation of the structural resonance of these bearings. This is, as noted, essential for envelope analysis. Further, because of the size, weight and cost of these types of bearings, there are few seeded fault tests conducted to learn about this type of bearing fault phenomenology.

3. LARGE SLOW BEARING EXAMPLE

This example is based on the availability of three commercial wind turbines (1.25 MW), where one of the turbines had a suspected main bearing fault. The machines were equipped with a bused condition monitoring system, which collected vibration data on two accelerometers mounted on the main bearing, and a tachometer signal. The accelerometer was based on microelectromechanical systems (MEMS) technology, where

- Accelerometer 1 has a bandwidth of 0 to 32 KHz, and a noise density of 4mg/√Hz, +/-70Gs.
- Accelerometer 2 has a bandwidth of 0 to 2.5 KHz, and a noise density of 110 µg/√Hz, +/-18Gs.

Each sensor was configured to sample at 3,052 sps for 120 seconds using a 24-bit analog-to-digital converter (ADC). The resampled spectrum in order domain for each machine is seen in Figure **3**. The order domain is the frequency divided by shaft rate. This is done to normalize each plot by the machine RPM. Each machine has a large spectral tone at order 89 (this is equivalent to 30.52 Hz), which is associated with the planetary gearbox mesh frequency.

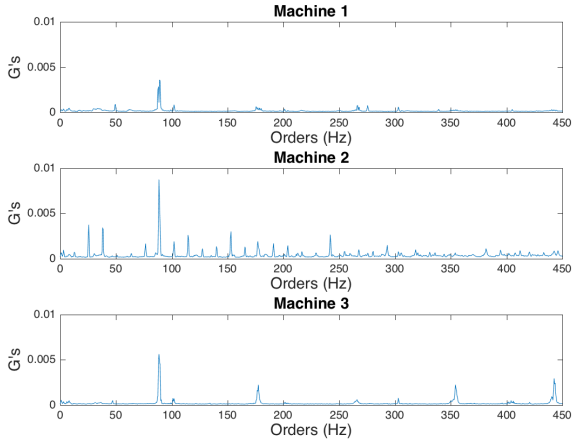

Figure 3. Resampled Spectrum in Order Domain.

Machine 2 shows multiple harmonics order 76 and 400 (26 and 140 Hz).

This is likely due to resonance. Investigating this, the envelope window was set from 50 to 150 Hz, i.e. bandwidth of 100 Hz, plotted in Figure **4** (zoomed to show 0 to 40 Hz). The window was selected above the gear mesh frequency. In Figure **4** Machine 2 shows an outer race fault, with multiple higher order harmonics associated with the outer race fault frequency. This fault characteristic is not present from machine 1 and 3, also depicted in Figure **4**. The fault energy in Machine 2 is approximately 10 times the noise density (e.g. floor energy) of Machine 1 and 3.

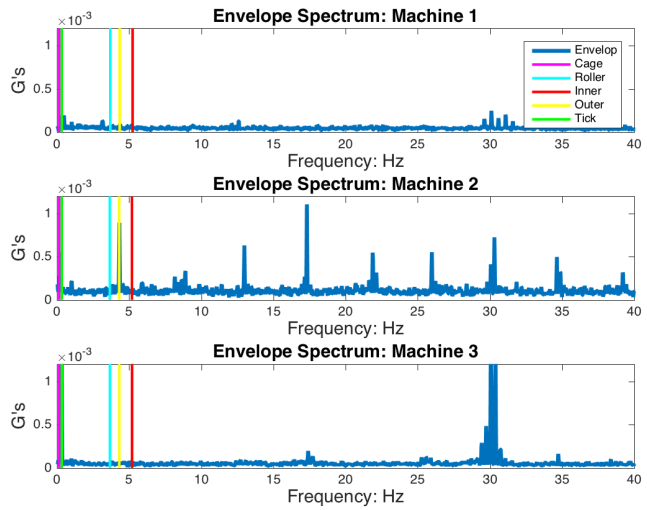

Figure 4. Envelope Spectrum Clearly Showing an Outer Rate Fault on Machine 2.

Note that after resampling the apparent sample rate is 5,580 sps, with a Nyquist of 2,760 Hz. The bandwidth of the window, being 100 Hz, allows a large decimation in time, by 27. Even with a modest 16,384 point FFT, this then allows a bin width of 0.0125 Hz. This gives enough resolution to resolve the cage fault from DC.

3.1. Cepstrum Analysis

The real cepstrum analysis was defined by Oppenheim (1965) and is a way to de-convolute homomorphic systems. The cepstrum is defined as:

$$cep = |\mathcal{F}^{-1}\{log(|\mathcal{F}\{f(t)\}|)\}|. \quad (6)$$

This is the real part of the inverse FFT of the log of the FFT. The concept is that the product of two signals is the sum of the logs of the signals. Since a bearing fault is the modulation of the fault frequency on the resonance frequency (e.g. multiplication of two signals), the cepstrum should be sensitive to this fault (Figure **5**). Because the inverse Fourier analysis has been called, the cepstrum is a time domain analysis. The x-axis of the analysis is called the quefrency (in seconds), and is the reciprocal of the frequency spacing.

For machine 2, the peak at quefrency of 0.231 presents a frequency of 4.3 Hz. This coincides with the outer race fault. For machine 3, the quefrency peak at 0.0346 represents a harmonic of 30 Hz. This is likely due to gear mesh and is not a feature of a bearing fault.

As the cepstrum is a time domain analysis, a number of condition indicators can be generated from it. For example the cepstrum kurtosis or cepstrum RMS could be used as a fault indicator. For this example, machine 3 generated large cepstrum RMS and kurtosis (see Table **1**), which is based on the average of 10 acquisitions. This information would not be actionable for the bearing fault, but may indicate a potential planetary gear ring fault.

Table 1. Cepstrum Condition Indicators.

Machine	Cepstrum RMS	Cepstrum Kurtosis
Machine 1	0.0038	63.33
Machine 2	0.0036	48.28
Machine 3	0.0045	98.42

It is felt that additional work needs to be performed on automated cepstrum analysis.

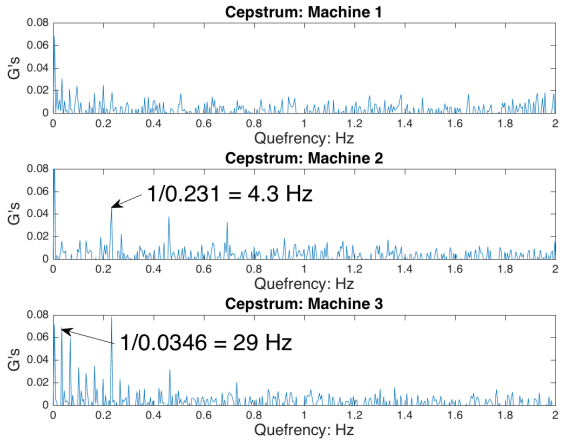

Figure 5. Cepstrum of the Main Bearings.

4. BEARING CONDITION INDICATORS AND HEALTH

For automated fault detection, a method is needed to both quantify the bearing damage and to recommend a maintenance action when appropriate. The quantification of damage is done using condition indicators (CI), which are descriptive statistics of the components under analysis. CIs for bearings include the energies associated with the bearing's fault pass frequencies f_{CPF}, f_{BFF}, f_{BPFI}, and f_{BPFO}. Other possible CIs are the average spectral energy, the spectral kurtosis (although more commonly used for window selection, see (Randall 2011), and the cepstrum RMS and Kurtosis. As an example, for a CI of the cage using Kurtosis, we take the FFT of the preprocessed vibration signal and the Kurtosis of the FFT resultant. Then we set the CI equal to the value of the Kurtosis of the FFT from the bin(s) associated with the f_{CPF}.

For this experiment, 16 acquisitions were available from Machine 1, nine acquisitions from Machine 2, and 15 from Machine 3. This allowed a population of CIs to be

developed for the cage, ball, and inner and outer race energies.

4.1. Threshold Setting and Component Health

Because the physics of failure is poorly understood (e.g. from a given CI value, the absolute level of damage cannot be calculated), threshold setting is typically a data driven process: maintenance is performed when a statistically set threshold is exceeded. The concept of thresholding was explored by Byington, Safa-Bakhsh, Watsen and Kalgren (2004) where for a given, single CI, a probability density function (PDF) for the Rician/Rice statistical distribution was used to set a threshold based on a probability of false alarm (PFA). This is contrasted with (Dempsey & Keller, 2008), where the relationship between CI threshold and PFA was explored to describe the receiver operating characteristics (ROC) of the CI for a given fault. Additionally, Dempsey used the ROC to evaluate the performance of the CI for a fault type. These methods support a data driven approach for condition monitoring by formalizing a method for threshold setting.

Because no single CI has been identified that works with all fault modes, the concept of fusing *n* number of CIs into a bearing health indicator (HI) was presented in (Bechhoefer, 2012). Computationally, the use of an HI is attractive. The HI provides decision-making tool for the end user on the status of the system health. The HI consists of the integration of several CIs into one value that provides the health status of the component to the end user.

Highlighted in (Bechhoefer, Duke & Mayhew, 2007) are a number of advantages of the HI over CIs, such as: controlling false alarm rate, improved detection, and simplification of user display. This approach allows the use of well established statistical methods. Further, it is a generalized process for threshold setting, where the HI is a function of distribution of CIs, regardless of the correlation between the CIs.

Prior to detailing the mathematical methods used to develop the HI, a nomenclature for component health is needed. To simplify presentation and knowledge creation for a user, a uniform meaning across all components in the monitored machine should be developed. The measured CI statistics (e.g. PDFs) will be unique for each component type (due to different rates, materials, loads, etc.). This means that the critical values (thresholds) will be different for each monitored component. By using the HI paradigm, one can normalize the CIs, such that the HI is independent of the component.

The HI can be designed such that there are two alert levels: warning and alarm. This paradigm also provides a common nomenclature for the HI, such that:

- The HI ranges from 0 to 1, where the probability of exceeding an HI of 0.5 for a nominal component (e.g. no damage) is the PFA.
- A warning alert is generated when the HI is greater than or equal to 0.75.
- An alarm alert is generated when the HI is greater than or equal to 1.0. Continued operations could cause collateral damage.

Note that this nomenclature does not define a probability of failure for the component, or that the component fails when the HI is 1.0. Rather, it suggests a change in operator behavior to a proactive maintenance policy: perform maintenance prior to the generations of cascading faults. For example, by performing maintenance on a bearing prior to the bearing shedding extensive material, costly gearbox replacement can be avoided.

4.1.1. Controlling for the Correlation Between CIs:

All CIs have a PDF. Any operation on the CI to form a HI is then a function of distributions. For this study, the HI function is taken as the norm of *n* CIs (energy).

In general, the correlation between CIs is non-zero. This correlation implies that for a given function of distributions to have a threshold that operationally meets the design PFA, the CIs must be whitened (e.g. de-correlated). Fukunaga (1990) presented a whitening transformation using the Eigenvector matrix multiplied by the square root of the Eigenvalues (diagonal matrix) of the covariance of the CIs: $\mathbf{A} = \mathbf{\Lambda}^{1/2}\,\mathbf{\Phi}^{\mathrm{T}}$, where $\mathbf{\Phi}^{\mathrm{T}}$ is the transpose of the Eigenvector matrix and Λ is the Eigenvalue matrix. The transformation is not orthonormal; the Euclidean distances are not preserved in the transformation. While ideal for maximizing the distance (separation) between classes (such as in a Bayesian classifier), the distribution of the original CI is not preserved. This property of the transformation makes it inappropriate for threshold setting.

If the CIs represented a metric, such as bearing energy, then an HI can be constructed, which is the square of the normalized power (e.g. square root of the squared acceleration). A generalized whitening solution can be found using Cholesky decomposition; see (Bechhoefer, He & Dempsey, 2011). The Cholesky decomposition of a Hermitian, positive definite matrix results in $\boldsymbol{A} = \boldsymbol{L}\boldsymbol{L}^{*}$, where $\boldsymbol{L}$ is a lower triangular, and $\boldsymbol{L}^{*}$ is its conjugate transpose. By definition, the inverse covariance ($\mathbf{\Sigma}^{-1}$) is a positive definite Hermitian. It then follows that if

$$\boldsymbol{L}\boldsymbol{L}^{*} = \mathbf{\Sigma}^{-1}, \tag{7}$$

where we have defined $\boldsymbol{A} = \mathbf{\Sigma}^{-1}$, then

$$\boldsymbol{Y} = \boldsymbol{L} \times \boldsymbol{C}\boldsymbol{I}^{\mathrm{T}}. \tag{8}$$

The vector ***CI*** is the correlated CIs used for the HI calculation, and ***Y*** is 1 to n independent CIs with unit variance (one CI representing the trivial case). The Cholesky decomposition, in effect, creates the square root of the inverse covariance. This in turn is analogous to dividing the CIs by their standard deviations (the trivial case of one CI). This creates the necessary independent and identical distributions required to calculate the critical values for a function of distributions.

4.1.2. HI Based on Rayleigh PDFs

The CIs for bearing energy (assuming nominal bearings) have Rayleigh like PDFs (e.g. heavily tailed). Consequently, the HI function was designed using the Rayleigh distribution. The PDF for the Rayleigh distribution uses a single parameter, β, defining the mean $\mu = \beta \times (\pi/2)^{0.5}$ and variance $\sigma^2 = (2 - \pi/2) * \beta^2$. The PDF of the Rayleigh is: $x/\beta^2 \exp(x/2\beta^2)$. Note that when applying these equations to the whitening process, the value for β for each CI will then be: $\sigma^2 = 1$, and $\beta = \sigma^2 / (2 - \pi/2)^{0.5} = 1.5264$.

The HI function using the norm of n CIs can be shown to define a Nakagami PDF (Bechhoefer & Bernhard, 2007). The statistics for the Nakagami are $\eta = n$, and

$\omega = 1/(2-\pi/2)*2*n$, where n is the number CIs used in the calculation of Y. The critical value for the HI, given four CIs were used (cage, ball, inner and outer race energy), so that: $\eta = 4$, and $\omega = 18.64$. For a PFA of 10^{-6}, the threshold 9.97, with the HI function calculated as:

$$HI = \frac{0.5}{9.97}\sqrt{\boldsymbol{Y}\boldsymbol{Y}^{\mathrm{T}}}. \qquad (9)$$

The 0.5 value normalized the HI, such that the probability of an HI being greater than 0.5 for a nominal bearing is 10^{-6}. The HI for the machines are given as in Figure **6**.

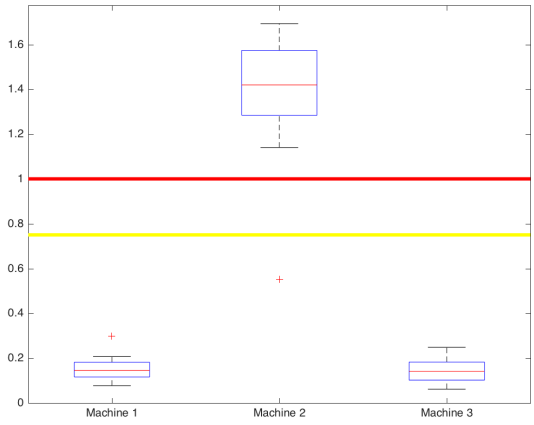

Figure 6. Main Bearing Health.

5. EFFECT OF ACCELEROMETER NOISE DENSITY

The prior analysis was conducted with accelerometer 2, with a noise density110 μg/√Hz. This is because there was no fault detection with accelerometer 1, with a noise density of 4mg/√Hz, i.e. accelerometer 1 had 36x (15.6 dB) the noise floor of accelerometer 2. By increasing the acquisition time by 4x, the signal to noise can be increased by 3 dB (2x). This is because the Welches spectrum averages the power, reducing random noise by $1/\sqrt{n}$, where n is the number of averages.

This was verified by increasing the data length to 480 seconds, and 960 seconds (4x or 3dB and 8x or 4.5 dB, Figure **7**).

Increasing the Signal to Noise by 3 dB allows the outer race fault to be detectable. The acquisition is eight minutes and 1,464,960 data points. This may exceed the memory of some embedded systems. Additionally, because of the large variation is speed seen over eight minutes, it necessitates the use of a time synchronous resampling algorithm (Bechhoefer et al., 2013).

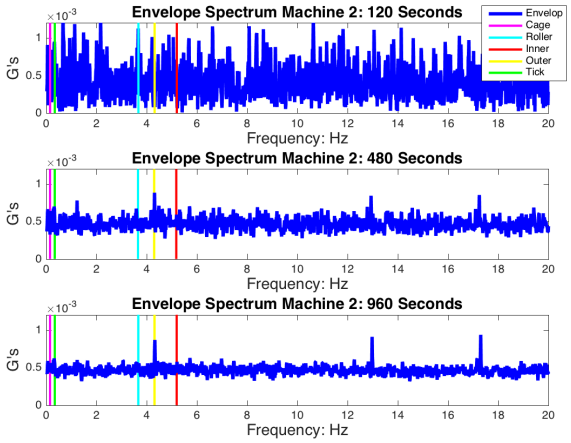

Figure 7. Reducing Noise by Increasing Sample Length.

6. OTHER CONDITION ANALYSIS TECHNIQUES

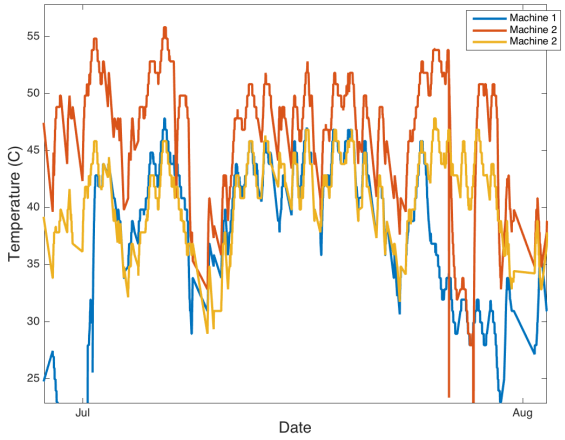

Figure 8. Main Bearing Temperature.

Both temperature, from the supervisory control and data acquisition (SCADA), and grease analysis was available for these machines. Temperature for machine 2 ran five to 10 degrees hotter than for the machine 1 and 3 (Figure **8**). This data was taken when all of the machines were generating more than 200 KW of power.

The grease analysis was performed by an ISO 9001:2008 and ISO/IEC 17025:2005 certified laboratory (Table **2**).

Table 2. Main Bearing Grease Analysis (ppm).

Aqueous Metals	Machine 1	Machine 2	Machine 3
Silver, Aq. ppm	<9.37	<10.98	<10.05
Aluminum, Aq. pp	<10.8	**268.5	**175.6
Boron, Aq. ppm	<7.9	<9.3	<8.5
Barium, Aq. ppm	<5.8	<6.8	<6.2
Calcium, Aq. ppm	*34.1	*43.1	<17.8
Cadmium, Aq. ppm	<5.8	<6.8	<6.2
Chromium, Aq ppm	<10.8	**136.4	**91.3
Copper, Aq. ppm	**71.5	**16483.0	**11679.7
Iron, Aq. ppm	121.8	**27499.3	**16084.7
Potassium, Aq. p	<14.4	<16.9	<15.5
Magnesium, Aq. p	<7.2	<8.4	<7.7
Manganese, Aq. p	<5.8	*171.3	*77.2
Molybdenum, Aq.	<13.0	39.8	<13.9
Sodium, Aq. ppm	<15.9	<18.6	<17.0
Nickel, Aq. ppm	<7.2	<8.4	<7.7
Phosphorus, Aq.	*<50.5	*991.2	*669.1
Lead, Aq. ppm	<31.7	**236.3	**132.0
Antimony, Aq. pp	<16.6	<19.4	<17.8
Silicon, Aq. ppm	20.7	**241.5	**147.2
Tin, Aq. ppm	<20.9	<24.5	<22.4
Titanium, Aq. pp	<3.6	<4.2	<3.9
Vanadium, Aq. pp	<3.6	<4.2	<3.9
Zinc, Aq. ppm	*134.6	*10629.7	*7173.2

The table is coded by the laboratory such that (*) yellow indicates a caution limit and (**) red is an alarm limit. Machine 2 had the highest level of aqueous metals in the grease. Machine 3 grease analysis indicates a fault, yet, machine 3 vibration health is nominal, i.e. not actually higher than machine 1.

7. CONCLUSION

The availability of both vibration, temperature and grease analysis from three wind turbines, where one turbine is suspected of having damaged main bearing, allows for an opportunity to develop a strategy for fault detection of large, slow bearings. Approximately ten acquisitions from two accelerometers (high bandwidth, high noise, and low bandwidth, low noise) and a tachometer were taken. Temperature was available from the SCADA system every ten minutes. Grease analysis from an ISO certified laboratory was also available from these machines.

In order to detect faults using vibration data, long acquisition times are needed (120+ seconds). Because of the long acquisitions, there were large changes in shaft speed. This is detrimental to the analysis because it smears the spectral content in the Fourier analysis. A time synchronous resampling algorithm used tachometer data to correct for changes in shaft speed, improving the analysis (the Fourier analysis assumes a stationary signal).

The envelope analysis was conducted using resampled vibration data (120 seconds at 3,052 sps) and a 50 to 150 Hz window with a 16,384-point spectrum. This facilitated the detection of an outer race fault on machine 2. Machine 1 and 3 were found to be normal. The fault was detected with the low noise density (110 $\mu g/\sqrt{Hz}$) sensor. The high noise density accelerometer could not detect the fault until the acquisition was increased to 480 seconds (3 dB improvement in SNR). The cepstrum analysis was performed on the vibration data, but the results were not actionable.

The main bearing's component health was calculated using a data driven method. Using the Nakagami distribution and a probability of false alarm of 10^{-6}, the bearing condition indicator data was mapped to a health indicator, where a health indicator of less than 0.5 is nominal, greater than 0.75 and less than 1 is warning, and greater than 1 is alarm. The

health indicator for the main bearing on machine 2 was 1.45.

Temperature data indicated that machine 2 ran 5 to 10 °C hotter than machine 1 and 3. The grease analysis indicated that both machine 2 and 3 were faulted, as many aqueous metals were in alarm.

Typically, vibration based detection on large slow bearings is difficult. However, using long acquisition times to improve resolution and proper window selection, the vibration data were easier to interpret, and gave more actionable information, than temperature and grease analysis. With online condition monitoring, using the trend of the health indicator, it is likely that remaining useful life of the bearing could be calculated. The vibration data, as presented, can give the operations and maintenance organizations valuable information to enhance logistic support of the machine.

ACKNOWLEDGEMENT

The research presented in this paper has received funding from the Norwegian Research Council, SFI Offshore Mechatronics, project number 237896.

REFERENCES

Bechhoefer, E., & Bernhard, A. (2007). A Generalized Process for Optimal Threshold Setting in HUMS. *IEEE Aerospace Conference, Big Sky*.

Bechhoefer, E., Duke, A., & Mayhew, E. (2007). A Case for Health Indicators vs. Condition Indicators in Mechanical Diagnostics. *American Helicopter Society Forum 63, Virginia Beach*.

Bechhoefer, E., He, D., & Dempsey, P. (2011). Gear Threshold Setting Based On a Probability of False Alarm. *Annual Conference of the Prognostics and Health Management Society*.

Bechhoefer, E., & He, D. (2012). A Process for Data Driven Prognostics, *MFPT*, Dayton, Ohio.

Bechhoefer, E., & Fang, A., (2012). Algorithms for Embedded PHM. *Prognostics and Health Management (PHM), IEEE*.

Bechhoefer, E. (2013). Condition Based Maintenance Fault Database for Testing Diagnostics and Prognostic Algorithms. *MFPT*.

Bechhoefer, E., Van Hecke, B., & He, D. (2013). Processing for Improved Spectral Analysis. *PHM Conference*.

Byington, C., Safa-Bakhsh, R., Watson, M., & Kalgren, P. (2003). Metrics Evaluation and Tool Development for Health and Usage Monitoring System Technology. *HUMS Conference*, DSTO-GD-0348.

Darlow, M.S., Badgley, R. H. & Hogg, G. W. (1974). *Application of high frequency resonance techniques for bearing diagnostics in helicopter gearboxes*. US Army Air Mobility Research and Development Laboratory, Technical Report pp. 74-76.

Dempsy, P. & Keller, J. (2008). *Signal Detection Theory Applied to Helicopter Transmissions Diagnostics Thresholds*. NASA Technical Memorandum 2008-215262.

Fukunaga, K. (1990). *Introduction to Statistical Pattern Recognition*. Academic Press, London, p. 75.

Ho, D. & Randall, R. B. (2000). Optimization of bearing diagnostic techniques using simulated and actual bearing fault signals. *Mechanical Systems and Signal Processing.* 14 (5), 763-788.

Oppenheim, A. V. (1965). *Superposition in a class of nonlinear systems* (Ph.D. dissertation). Res. Lab. Electronics, Massachusetts Institute of Technology, Cambridge, MA.

Randall, R. (2011). *Vibration-based Condition Monitoring: Industrial, Aerospace & Automotive Application*. John Wiley, New York.

BIOGRAPHIES

Eric Bechhoefer is the president of GPMS, Inc., a company focused on the development of low-cost condition monitoring systems. Dr. Bechhoefer is the author of over 100+ juried papers on condition monitoring and prognostics health management, and holds 23 patents in the field of CBM.

Rune Schlanbusch received his MSc in Space Technology from Narvik University College (NUC), Norway in 2007, and a PhD in Engineering Cybernetics from NTNU, Norway in 2012. He currently holds positions as Senior Researcher at Teknova, Norway and II Associate Professor at Department of Technology, NUC.

Tor Inge Waag works as Specialist Engineer at MHWirth AS and holds a part time position as Senior Researcher at Teknova AS in Norway. He has received both his MSc and PhD in Physics from NTNU, Norway. His primary work focus is at present on prognostics and health management, signal processing, and condition monitoring.